

Dodecagonal Quasicrystalline Morphology in a Poly(styrene-*b*-isoprene-*b*-styrene-*b*-ethylene oxide) Tetrablock Terpolymer

Jingwen Zhang and Frank S. Bates*

Department of Chemical Engineering and Materials Science, University of Minnesota, Minneapolis, Minnesota 55455, United States

ABSTRACT: A dodecagonal quasicrystalline (QC) morphology is identified in a poly(styrene-*b*-isoprene-*b*-styrene-*b*-ethylene oxide) (SISO) tetrablock terpolymer based on evidence provided by transmission electron microscopy (TEM), small-angle X-ray scattering, and dynamic mechanical spectroscopy measurements. The QC state occurs at temperatures between those associated with simple hexagonal order (HEX) and the σ -phase ($P4_2/mnm$), $T_{\text{HEX}} < T_{\text{QC}} < T_{\sigma} < T_{\text{ODT}}$, where T_{ODT} is the order–disorder transition temperature. All three morphologies are formed from spherical domains containing an O core surrounded by a shell of S that screens unfavorable segment–segment interactions with an I-rich matrix. TEM analysis reveals a QC morphology with 12-fold rotational symmetry but devoid of long-range translational order, along with locally coordinated structures consistent with dodecagonal quasicrystalline approximants. The SISO molecular architecture decouples control over the domain shape and interdomain interactions, leading to a multiplicity of packing symmetries.

Quasicrystals, discovered just 28 years ago, have disrupted traditional assumptions regarding the periodic placement of atoms and molecules in two- and three-dimensional Cartesian spaces. Landmark publications by Shechtman and co-workers^{1–3} first demonstrated that certain metal alloys could spontaneously assemble into unusual structures characterized by rotational symmetry but without long-range translational order. Such aperiodic arrangements can accommodate local packing geometries that are unfeasible based on conventional crystalline order (i.e., with the standard 230 space groups) including icosahedral and dodecagonal symmetries. Quasicrystalline order can be visualized and appreciated using Penrose tiling patterns (first identified in the 1970s), generated by ensembles of rhombuses with aspect ratios linked by the “golden ratio”. However, these simple geometric constructions do not illuminate the underlying interatomic and intermolecular interactions responsible for producing 5-, 8-, 10-, and 12-fold rotational symmetry in a slew of alloys^{4–12} and naturally occurring^{13,14} inorganic compounds and a few organic materials.^{15–17}

Recently we reported the self-assembly of sphere-forming diblock and tetrablock polymers into the σ -phase,¹⁸ a quasicrystal approximant characterized by a large tetragonal unit cell ($P4_2/mnm$ space group symmetry) containing 30 spheres, each formed by hundreds of macromolecules. This discovery, along with reports of similar phase behavior in certain types of dendrimers,¹⁵ supports the notion that

particle–particle interactions between soft objects mediated by elastic (entropy-based) deformations at constant overall density may be uniquely tunable, affording access to new and potentially useful crystalline and quasicrystalline states. ABA'C type tetrablock terpolymers are particularly attractive for this purpose since the basic domain geometry (e.g., spherical) and interparticle interactions can be (at least partially partially) decoupled.

The thermodynamic driving force for block segregation is governed by the segment–segment interaction parameters, χ_{AB} , χ_{AC} , and χ_{BC} , the composition, and the overall molecular weight.¹⁹ When $\chi_{\text{BC}} > \chi_{\text{AB}} \approx \chi_{\text{AC}}$, contact between the B and C blocks is unfavorable leading to domain structures that avoid B/C interfaces. Judicious choice of the length of the C blocks, N_{C} , relative to N_{A} , N_{A} , and N_{B} , offers control over the domain curvature (e.g., spherical or cylindrical domains), while the magnitude of $\chi_{\text{AB}} \approx \chi_{\text{AC}}$ and $\xi = N_{\text{A}}/N_{\text{A}}$ and the overall block polymer size, $N = \sum N_i$, dictate the morphology of the surrounding matrix. This communication reports the formation of a dodecagonal quasicrystalline morphology in a sphere-forming poly(styrene-*b*-isoprene-*b*-styrene-*b*-ethylene oxide) (SISO) tetrablock terpolymer ($\xi = 1$) at temperatures intermediate to those leading to a low-temperature (simple) hexagonal phase²⁰ and the σ -phase at high temperatures, prior to disordering.

A tetrablock terpolymer denoted SISO-2 (see Figure 1a) was synthesized using a two-step anionic polymerization method

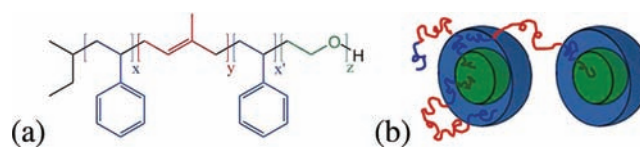


Figure 1. (a) Molecular structure of SISO tetrablock terpolymer and (b) core–shell spherical morphology. Unfavorable interactions between the O (core) and I (matrix) blocks are screened by S blocks (shell).

and characterized as reported in a previous publication.²⁰ This compound has a number average molecular weight $M_n = 24.4$ kg/mol and dispersity index $M_w/M_n = 1.04$ and contains 35% by volume poly(styrene) (divided equally between the two S blocks), 56% I, and 9% O (each $\pm 1\%$). Volume fractions were calculated based on ¹H NMR analysis and using published homopolymer densities at 140 °C: $\rho_{\text{I}} = 0.830$, $\rho_{\text{S}} = 0.969$, and $\rho_{\text{O}} = 1.064$ g/mol.²¹ As detailed in an earlier report,²⁰ this combination of composition and molecular weight leads to the

Received: March 5, 2012

Published: April 16, 2012

formation of spherical domains with a core of O blocks (melting temperature $T_{m,O} \approx 38$ °C) surrounded by a S-rich corona (glass transition temperature $T_{g,S} \approx 90$ °C) embedded in a S/I matrix (glass transition temperature $T_{g,I} \approx -70$ °C) as illustrated in Figure 1b. At 120 °C these spherical domains appear to be organized on a simple hexagonal lattice,²⁰ to the best of our knowledge a unique crystal structure for a collection of uniformly sized spheres. (Several other SISO specimens with larger O blocks also display this morphology). We selected SISO-2 for additional study due to its proximity to the order–disorder transition (ODT) (reducing the O content leads to a homogeneous material); dynamical mechanical spectroscopy (DMS) and small-angle X-ray scattering (SAXS) experiments revealed that the order–disorder transition occurs at $T_{ODT} = 212 \pm 3$ °C.

Evidence of additional ordered phases in SISO-2 at elevated temperatures was provided by isochronal DMS measurements ($\omega = 1$ rad/s) while heating and cooling the material at 2 °C/min. Figure 2 shows a significant rise in the dynamic elastic

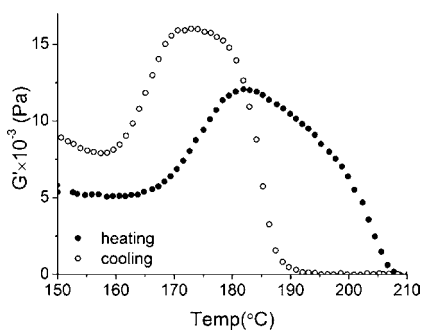


Figure 2. Linear dynamic elastic shear modulus G' for SISO-2 determined while heating and cooling at 2 °C/min at a frequency of $\omega = 1$ rad/s. Changes in $G'(T)$ beginning at 165 and 200 °C while heating and loss of elasticity at 210 °C are interpreted as order–order and order–disorder transitions, respectively. Hysteresis in $G'(T)$ is indicative of first-order phase transitions.

modulus G' upon heating, beginning at about 165 °C, which we associate with an order–order transition (OOT).²² A second less dramatic change in $G'(T)$ occurs at about 200 °C, and by approximately 210 °C, the elastic response of the material has dropped below the resolution of the instrument. Frequency scans taken at $T > 210$ °C (not shown) are consistent with a liquid-like viscoelastic response, which we associate with a state of disorder. Upon cooling, $G'(T)$ rises then falls again, although both transitions occur at lower temperatures, consistent with the hysteresis associated with first-order phase transitions.

We have probed the structure of SISO-2 between 120 and 215 °C using synchrotron SAXS conducted at the Argonne National Laboratory (DND-CAT located at Sector 5 at the Advanced Photon Source (APS)). SAXS specimens were annealed under vacuum at 120 °C for 24 h, then cooled and sectioned into small (ca. 0.02 g) pieces and mounted between Kapton windows in a temperature regulated (± 1 °C) sample cell (a modified differential scanning calorimeter) and purged with helium. Cylindrically symmetric powder scattering patterns were collected on a Mars area detector and reduced to the one-dimensional form of intensity versus scattering wave vector, $q = 4\pi\lambda^{-1}\sin(\theta/2)$, where $\lambda = 0.0729$ nm was the radiation wavelength and θ is the scattering angle. A series of SAXS experiments was conducted after holding the specimen at a targeted temperature for 5 min; measurements were repeated

every 5 min until no change in the response was detected (typically 3 or more patterns were recorded at each temperature).

Selected SAXS results are shown in Figure 3. At 120 °C distinct diffraction peaks are evident at relative positions ($q/$

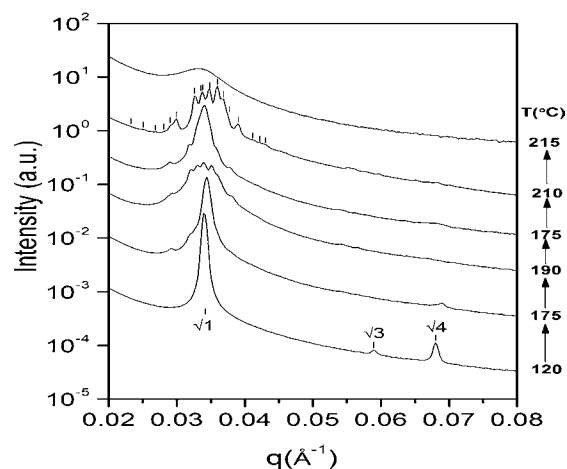


Figure 3. Representative synchrotron SAXS data obtained from SISO-2. Hexagonal and tetragonal (σ -phase) order and disorder are identified with the results at 120, 210, and 215 °C, respectively. Relative σ -phase peak positions, reported previously for another SISO material,¹⁸ are identified with the 210 °C scattering pattern. A distinctly different structure is indicated by the thermally reversible scattering patterns obtained at 175 °C. The data have been shifted vertically for clarity.

$q^*)^2 = 1, 3, 4$, where q^* represents the first-order reflection, consistent with an ordered state with hexagonal symmetry. Increasing the temperature to 175 °C leads to the appearance of at least four new reflections, two below and two above the principal peak, and loss of the peak corresponding to $\sqrt{3}q^*$ at 120 °C. Increasing the temperature further, to 190 °C, produces dramatic changes in the scattering around q^* , accompanied by the appearance of additional (weak) peaks at higher q . Cooling back to 175 °C reverses these changes. Subsequent heating to 210 °C results in a distinctive set of reflections that exactly match the scattering pattern for the σ -phase as shown earlier.¹⁸ Finally, at 215 °C all the Bragg peaks disappear, replaced by a single broad scattering maximum centered at q^* , which we interpret as correlation hole scattering from the disordered material. Additional SAXS experiments, performed while heating and cooling SISO-2 at various rates between 120 and 215 °C, lead us to conclude that a structure distinct from the hexagonal and tetragonal (σ -phase) states is present between about 160 and 190 °C, although the associated scattering patterns lack sufficient detail to permit identification of the related morphology.

We have employed transmission electron microscopy (TEM) in order to establish the morphology of the low- and intermediate-temperature structures identified by SAXS. Specimens were annealed in a vacuum oven for 1 day at 120 and 175 °C, then plunged into liquid nitrogen to preserve each morphology; vitrification of poly(styrene) below about 90 °C fixes the quenched morphology, even after heating back up to room temperature. Thin sections (ca. 70 nm) were obtained by cryo ultramicrotoming pieces of the material following rough facing and staining with the vapor from a 5% osmium tetroxide aqueous solution; OsO_4 reacts preferentially with the poly-

(isoprene) blocks providing electron density contrast. Figure 4 illustrates representative micrographs obtained using a Tecnai

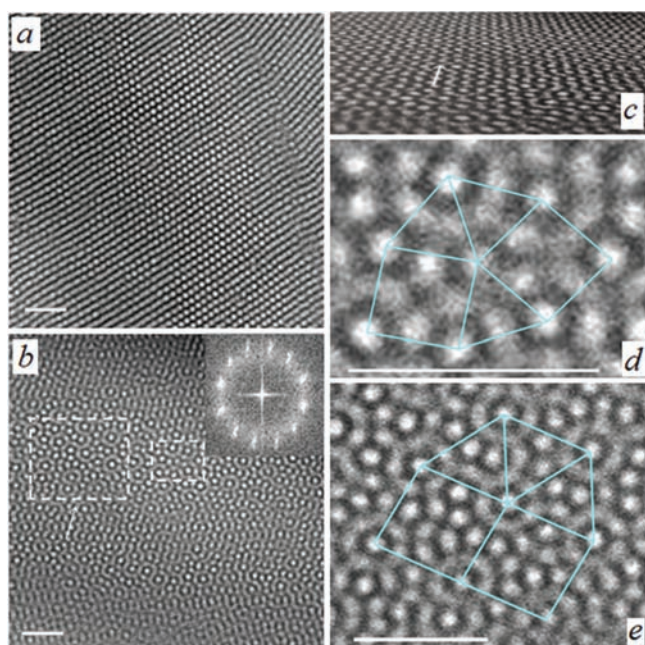


Figure 4. TEM micrographs obtained from OsO₄ stained SISO-2 tetrablock terpolymer after annealing for one day at (a) 120 and (b) 175 °C. Both images are formed by spherical domains containing a core of O blocks. Long-range order in (a) is consistent with simple hexagonal (P_6/mmm) packing, as shown previously.²⁰ The morphology in (b) contains clear evidence of local (ca. 50–100 nm) coordination of spheres but lacks long-range translational order. The scale bars represent 100 nm. A Fourier transform (inset) reveals 12-fold rotational symmetry consistent with dodecagonal quasicrystalline order. Rotating the image (b) out of the plane of view reveals planes of (uncorrelated) spheres as seen in (c); the arrow identifies the orientation. Clusters displaying σ and H quasicrystal approximant tiling, located within the dashed boxes in (b), are magnified and highlighted in (d) and (e), respectively.

T12 instrument (University of Minnesota Characterization Facility) operating at 120 kV. The image obtained from the specimen annealed at 120 °C (Figure 4a) shows spherical domains (approximately 13 nm in diameter) arranged with long-range translational order; our previous analysis suggests a simple hexagonal crystal structure (P_6/mmm symmetry) for this specimen at this temperature.²⁰

The micrograph shown in Figure 4b, derived from the specimen annealed at 175 °C, is qualitatively different. (Here we note that images similar to the one shown in Figure 4b were identified in other regions of the TEM specimen and reproduced in other specimens prepared in the same manner. However, this morphology was not represented in the majority of the images obtained from this material as discussed below.) Spherical domains (the same diameter as those found in Figure 4a) appear to be distributed with distinctive local coordination, characterized by cylindrical columns of spheres (approximately 35 nm in diameter) that surround stacks of individual spherical domains. This motif resembles the basic structural unit characterizing the σ -phase.¹⁸ Although clearly lacking long-range translational order, this morphology contains 12-fold rotational symmetry as demonstrated by the Fourier transform (inset to Figure 4b), consistent with a dodecagonal quasicrystal-

line morphology. We have rotated the TEM image shown in Figure 4b out of the plane of view, which illustrates the origins of the 12-fold rotational order. Parallel planes of (uncorrelated) spheres are evident along the indicated direction in Figure 4c, and similar images are obtained upon sequential rotations of $360^\circ/12 = 30^\circ$ around the normal to Figure 4b.

Careful examination of Figure 4b, and other similar images (not shown), reveals elements of intermediate scale structure that support our assignment of a quasicrystalline morphology. Ordered quasicrystal approximants are characterized by morphologies containing periodic two-dimensional Archimedean tiling formed from triangular and square elements; the σ -phase contains a distinctive pattern of $3^2\cdot 4\cdot 3\cdot 4$ elements. Dodecagonal quasicrystals are characterized by irregular tiling patterns that include mixtures of different approximants. Figure 4d,e highlights two such examples: a σ element ($3^2\cdot 4\cdot 3\cdot 4$) and a H element,^{23,24} respectively. Interestingly, these two approximants reflect tiling on different length scales (one versus two cylindrical column diameter spacing), another characteristic feature of quasicrystalline order.

Based on this analysis we believe that SISO-2 forms a two-dimensional dodecagonal quasicrystalline state at 175 °C; this pattern is replicated periodically in the layer normal direction.¹⁵ Consistent with this assignment, we have recorded other TEM images from this material showing regions with translational order, quasicrystalline order, and no apparent order. Assuming a polydomain texture, with a random distribution of grain orientations, the probability of slicing thin sections suitably oriented to exhibit the morphology seen in Figure 4b should be low, consistent with our observations.

While the geometric and space filling factors associated with quasicrystals are now well established, the interparticle interactions responsible for coordinating atomic, molecular, and supramolecular clusters with local icosahedral or dodecahedral symmetry remain elusive. Frank and Kasper²³ first pointed out the feasibility of creating a fascinating class of crystals (“Frank–Kasper” phases) built up from close-packed tetrahedral units of uniformly sized spheres that tile space with a host of packing symmetries, including $P4_2/mmm$ (σ -phase), $Pm3\bar{n}$, and $Fd3\bar{m}$. In 1992 Dzugutov²⁵ proposed an unusual interparticle pair potential with conventional short-range (hard core) repulsion and nearest-neighbor attraction (similar in form to the Lennard-Jones potential with a minimum at $r = 1.13\sigma$) augmented with long-range repulsion peaking at $r = 1.63\sigma$. The long-range repulsive portion of the potential frustrates conventional crystallization facilitating glass formation, and surprisingly dodecagonal quasicrystals,^{26,27} and the associated crystal approximants including several Frank–Kasper phases.²⁵ Figure 4b is strikingly similar in appearance to molecular simulations of dodecagonal quasicrystals in dense ensembles of spherical particles governed by the Dzugutov potential function.²⁴

Ungar and Zeng have argued that certain forms of soft materials, including lyotropic liquid crystals and dendrimers, should be susceptible to forming tetrahedral clusters, hence quasicrystals and Frank–Kasper phases.²⁸ SAXS experiments have revealed the sequence of phases $QC \rightarrow P4_2/mmm \rightarrow$ isotropic in certain supramolecular dendrimers,¹⁵ which has been attributed to molecular packing frustration.²⁸ This effect is well-established in single component block polymer melts, where stretching and compressing blocks away from preferred random-walk configurations is required in order to place domains (e.g., spheres) on an ordered lattice at uniform

polymer density.²⁹ In the mean-field limit diblock copolymer spheres order on a BCC lattice.^{30,31} However, recently we have shown that low molecular weight diblocks can form the σ -phase, presumably reflecting modified interdomain interactions due to non-Gaussian corona block chain statistics.¹⁸

ABA'C type tetrablock terpolymers in general, and SIS'O in particular, are especially attractive candidates for exploring new states of order in soft materials.³² Formation of spherical O cores, screened from unfavorable contact with I by the S' blocks (see Figure 1b), can be largely decoupled from the spatial arrangement of I and S segments in the surrounding matrix, offering direct control over the effective particle–particle interaction potential. Chemically dissimilar matrix blocks can be designed to produce uniform mixing, partial segregation (as with SISO-2), or complete microphase separation, by adjusting the individual block molecular weights. Varying the molecular symmetry parameter $\xi = N_S/N_I$ provides morphological control at constant overall composition. While we have not established cause and effect relationships between the tetrablock terpolymer molecular parameters (χ_{IS} , N_I , N_S , and ξ) and the occurrence of Frank–Kasper and QC phases, the results presented in this communication offer clues that will stimulate additional experimental and theoretical investigations.

AUTHOR INFORMATION

Corresponding Author

bates001@umn.edu

Notes

The authors declare no competing financial interest.

ACKNOWLEDGMENTS

This work was supported by the U.S. DOE, BES Division of Material Science and Engineering contract DEAC05-00OR22725 with UT-Battelle, LLC at Oak Ridge National Laboratory. The University of Minnesota Materials Research Science and Engineering Center (MRSEC) provided support for certain facilities. Use of the APS was supported by the U.S. DOE Office of Science, BES, under contract DE-AC02-06CH11357.

REFERENCES

- (1) Shechtman, D.; Blech, I.; Gratias, D.; Cahn, J. W. *Phys. Rev. Lett.* **1984**, *53*, 1951.
- (2) Cahn, J. W.; Shechtman, D.; Gratias, D. *Mater. Res.* **1986**, *1*, 13.
- (3) Levine, D.; Steinhardt, P. J. *Phys. Rev. Lett.* **1984**, *53*, 2477.
- (4) Ishimasa, T.; Nissen, H.-U.; Fukano, Y. *Phys. Rev. Lett.* **1985**, *55*, 511.
- (5) Rajasekharan, D.; Akhtar, D.; Gopalan, R.; Muraleedharan, K. *Nature* **1986**, *322*, 528.
- (6) Wang, N.; Chen, H.; Kuo, K. *Phys. Rev. Lett.* **1987**, *59*, 1010.
- (7) Tsai, A. P.; Inoue, A.; Masumoto, T. *Jpn. J. Appl. Phys.* **1987**, *26*, L1505.
- (8) Luo, Z.; Zhang, S.; Tang, Y.; Zhao, D. *Scr. Metall. Mater.* **1993**, *28*, 1513.
- (9) Tsai, A. P. *Sci. Technol. Adv. Mater.* **2008**, *9*, 013008.
- (10) Wang, J. F.; Mueller, M.; Wang, Z. G. *J. Chem. Phys.* **2009**, *130*, 154902.
- (11) Janot, C. *Quasicrystals: A Primer*, 2nd ed.; Oxford University Press: New York, 1994.
- (12) DiVincenzo, D. P.; Steinhardt, P. J. *Quasicrystals: The State of Art*; World Scientific: Singapore, 1991.
- (13) Bindi, L.; Steinhardt, P. J.; Yao, N.; Lu, P. J. *Science* **2009**, *324*, 5932.
- (14) Steinhardt, P. J.; Bindi, L. *Philos. Mag.* **2011**, *91*, 2421.
- (15) Zeng, X.; Ungar, G.; Liu, Y.; Percec, V.; Dulcey, A. E.; Hobbs, J. K. *Nature* **2004**, *428*, 157.
- (16) Hayashida, K.; Dotera, A.; Takano, A.; Matsushita, Y. *Phys. Rev. Lett.* **2007**, *98*, 195502.
- (17) Ceolin, R.; Agafonov, V.; Fabre, C.; Rassat, A.; Dworkin, A.; Andre, D.; Szwarc, H.; Schierbeek, A. J.; Bernier, P.; Zahab, A. J. *Phys. (Paris)* **2004**, *428*, 157.
- (18) Lee, S.; Bluemle, M. J.; Bates, F. S. *Science* **2010**, *330*, 349.
- (19) Bates, F. S.; Fredrickson, G. H. *Phys. Today* **1999**, *52*, 32.
- (20) Zhang, J.; Sides, S. W.; Bates, F. S. *Macromolecules* **2012**, *45*, 256.
- (21) Fetters, L. J.; Lohse, D. J.; Richter, D.; Witten, T. A.; Zirkel, A. *Macromolecules* **1994**, *27*, 4639.
- (22) Hillmyer, M. A.; Bates, F. S.; Almdal, K.; Mortensen, K.; Ryan, A. J.; Fairclough, J. P. A. *Science* **1996**, *271*, 976.
- (23) Frank, F. C.; Kasper, J. S. *Acta Crystallogr.* **1959**, *12*, 483.
- (24) Keys, A. S.; Glotzer, S. C. *Phys. Rev. Lett.* **2007**, *99*, 235503.
- (25) Dzugutov, M. *Phys. Rev. A* **1992**, *46*, R2984.
- (26) Dzugutov, M. *Phys. Rev. Lett.* **1993**, *70*, 2924.
- (27) Doye, J. P. K.; Wales, D. J.; Zetterling, F. H. M.; Dzugutov, M. J. *Chem. Phys.* **2003**, *118*, 2792.
- (28) Ungar, G.; Zeng, X. *Soft Matter* **2005**, *1*, 95.
- (29) Matsen, M. W.; Bates, F. S. *Macromolecules* **1996**, *29*, 7641.
- (30) Leibler, L. *Macromolecules* **1980**, *13*, 1602–1617.
- (31) Bates, F. S.; Cohen, R. E.; Berney, C. V. *Macromolecules* **1982**, *15*, 589.
- (32) Bates, F. S.; Hillmyer, M. A.; Lodge, T. P.; Bates, C. M.; Delaney, K. T.; Fredrickson, G. H. *Science* **2012**, *336*, 434.